



Stability of Column Rebar Cages for Buildings under Construction

Cliff D. Bishop¹, Patxi Uriz², Brian McDonald³

Abstract

The erection and bracing of column rebar cages are often left to the means and methods of the contractor, rarely under the guidance of a professional engineer. The cage is in its most vulnerable state before the formwork is erected and concrete is cast and set, sometimes resulting in buckling and collapse. In addition to the potential life-safety concerns, such collapses can cause significant delays due to damage of embedded steel. Unfortunately, numerous aspects specific to reinforcing cages make accurate predictions of stability limits difficult: the connection of the cage at its base (boundary conditions), transverse reinforcing bar size and spacing, tie wires used to fasten the transverse reinforcing bars to the longitudinal reinforcing bars, and effects of the reinforcement-to-concrete ratio. This paper uses solutions based on robust finite element analysis to validate simpler approaches to modeling column reinforcing cages. Finally, design methods are recommended to help prevent future failures.

1. Introduction

Column reinforcement cages are constructed, usually on the ground at the site or assembled elsewhere, by connecting longitudinal and transverse reinforcing bars together using thin, cold-drawn tie wire. After the cage is complete on the ground, the cage is then lifted into place using a crane. Finally, workers apply external bracing to the cage in order to hold it plumb during the placing of formwork and eventually, the casting of concrete. One such example of several in-situ column cages is shown in Fig. 1, whereas Fig. 2 shows close-ups of one column cage in particular.

¹ Ph.D., Associate, Exponent Inc., cbishop@exponent.com

² Ph.D., P.E., Managing Engineer, Exponent Inc., puriz@exponent.com

³ Ph.D., P.E., S.E., Principal Engineer, Exponent Inc., bmcdonald@exponent.com



Figure 1: Column cages during construction with partial-height concrete



(a)



(b)

Figure 2: Close-ups of a column rebar cage during construction

As evidenced by Fig. 2b, the amount of tightly-spaced reinforcing bar in any given column cage can be quite significant, especially if the building is constructed in regions of high seismicity. The American Concrete Institute's Building Code Requirements for Structural Concrete (ACI 318-11), as a referenced standard of the 2012 International Building Code (IBC 2012), provides the requirements for details of reinforcement including:

- Size and spacing of longitudinal reinforcement,
- Minimum and maximum ratios of longitudinal reinforcement area to concrete area (known as ρ in ACI 318),

- Size, spacing, and layout of transverse reinforcement including minimum bend diameters or rectangular versus spiral shapes, and
- Clear distances between the face of the concrete column and the face of the reinforcing bar.

Most of these factors for structural column reinforcement as detailed in Chapter 7 (Details of Reinforcement) of ACI 318-11 are updated with further restrictions when dealing with areas subject to higher seismic demands; ACI provides the more stringent requirements in Chapter 21 (Earthquake Resistant Structures).

2. Background

Stability for concrete structures is considered by ACI 318-11 only for the completed members and systems; i.e., after the concrete has already been cast and set. While these requirements may suffice to satisfy global stability of the system during the majority of its service life, they may not be good predictors of potential instabilities of column cages during construction.

2.1 Vulnerability of Column Rebar Cages

As is usually the case for buildings under construction, the stability of elements before the engineered system has been completed is often left to the means and methods of the contractor, who may not typically consult a professional engineer. As discussed in Section 1, there are a number of variables that contribute to the complex geometry of any column reinforcing cage. Also, any given project may have many different column cage types. As such, some jobs may have tall slender column cages with relatively little lateral ties between longitudinal bars. Rigorous stability analysis of these conditions is rarely considered practical by contractors with a history of good cage performance using empirical means of column bracing.

There have been over fifty reported failures of column rebar cages for bridges between 1995 and 2010 in the state of California alone (Builes-Mejia 2010). Builes-Mejia (2010) notes that most collapses occur under the following conditions:

1. Column cages with fixed bases,
2. Accidental loads and/or loss/removal of temporary support systems, and
3. The absence of bracing internal to the column cage.

While these observations were noted by Builes-Mejia for columns from bridges, the authors' personal experience includes building column rebar cage collapses under similar scenarios. Fig. 3 and Fig. 4 show examples of building column cage failures investigated by the authors.

Cage collapse can have disproportionate effects on the construction process. Not only is the potential for cage collapse a safety concern for the workers on-site, there is also the need to consider other repercussions:

- Potentially extreme schedule delays due to:
 - Federal/state accident investigations, by e.g., the Occupational Safety and Health Administration (OSHA),
 - Repair of the damaged cage and potential replacement of embedded bars,
 - Insurance-related investigations by outside consultants, and
 - Review of all cage designs by a registered design professional of responsible charge.
- Potentially expensive litigation for damage to victims or schedule delays, and

- Development of a poor safety reputation for the rebar fabricator, sub-contractors, or the general contractor.



Figure 3: Collapsed column rebar cage example 1



Figure 4: Collapsed column rebar cage example 2

2.2 Toward a Column Reinforcing Cage Stability Assessment

The authors posit that if simplified methods were available to quickly evaluate column cage stability, then more installations would be constructed based on engineered design rather than convention or contractor means and methods. Specifically, given the nature of cage fabrication, it is not always obvious how one might determine the section properties of the cage (e.g., accounting for the partial composite action realized by connecting the longitudinal and transverse reinforcing using tie wire); the applied loading that is consistent with the physical geometry; the

effectiveness of bracing (both internal and external to the cage); and consistent boundary conditions. Ultimately, it is these simplified models which are sought.

Section 1 gave an overview of column reinforcing cages and detailed many of the variables which affect their geometry. Section 2 discussed the propensity for cage collapse and presented a number of the observations from actual failures. The rest of the paper is organized as follows: Section 3 provides the details of virtual experiments in which various column cage geometries are postulated and analyzed. Section 4 provides the results from the virtual experiments and discussion. Finally, Section 5 generalizes the results into a set of simple, cohesive recommendations for engineers to analyze cages during construction.

2.3 Prior Work on Reinforcing Cage Stability

Professor Ahmad Itani in the Department of Civil & Environmental Engineering at the University of Nevada, Reno has spearheaded many experiments, papers, and presentations centered on bridge column cage stability during construction for the State of California's Department of Transportation (Caltrans). One major body of work concerning rebar cage stability is by Builes-Mejia, Itani, and Sedarat (2010). Their report investigated bridge column cage collapses through experimental and analytical work. They varied parameters including the tie wire connections, internal bracing, column diameter, longitudinal and transverse reinforcement ratios, and column height for cages subjected to lateral loads. Ultimately, their findings suggest that the internal bracing was a major contributor to cage stability. Furthermore, conventional means and methods of column cage bracing are nicely summarized in Casey (2013).

3. Research Methodology

This section details the modeling of relevant physical characteristics and how they are varied throughout different analyses to assess column cage stability. The many geometric variables and overall system complexity prove difficult to simplify. The ultimate goal of this work is to demonstrate that simple models are available to assess cage stability, hopefully encouraging more analyses of these systems in the future.

3.1 Model Description and Varied Parameters

3.1.1 Column Geometry and Reinforcement

All columns analyzed in this paper have a height equal to thirty feet. The two column cage longitudinal reinforcing layouts selected for analysis and presented herein are composed of either (8)-#10 bars or (16)-#8 bars. The reinforcement ratio (ρ) is either 2% or 4%. Since the area of column longitudinal steel remains the same as ρ is varied, this necessitates the change in the overall column dimensions and bar spacing between analyses. Fig. 5 shows cross-sections of the four reinforcement layouts: (8)-#10 with ρ equal to 2% and 4% and (16)-#10 with ρ equal to 2% and 4%. All transverse reinforcing bars are #4 with varying spacing along the height of the column and lengths that vary based on the spacing of the column longitudinal bars. The overall cage weight including the longitudinal and transverse reinforcing is shown in Table 1. It should be noted that the weight of the transverse reinforcing is double what is shown graphically for the 16-bar configuration shown in Fig. 5c and Fig. 5d. This is meant as a rough approximation to account for additional transverse bar weight that may be required throughout the cross-section to

satisfy ACI requirements, especially in regions of high seismicity. Although the transverse steel weight is doubled, the additional tie wire connections for the assumed extra transverse bars are conservatively neglected in these analyses.

Composite action or the transfer of shear between individual reinforcing bars in the longitudinal direction greatly increases the stability of the reinforcing cage. As will be shown later, the effective moment of inertia of a cross section with fully composite behavior can be orders of magnitude larger than that of the individual bars. Reinforcing cages develop partial composite action through the mechanical tie wire connectors between the longitudinal bars and the transverse reinforcement. A sophisticated analysis, one chosen to closely mimic the physical system, could model each bar and each tie to attempt the most-realistic assessment of cage capacity. This method of analysis is computationally inefficient and may take many hours to develop a single model, and the cost of providing additional bracing may prove less expensive than engineering time. As such, simple modeling procedures are required to quickly assess safety. A much simpler and more conservative model is available whereby the summed moments of inertia and areas of each individual longitudinal bar are simply lumped into a line model, i.e., transverse reinforcing and the ties do not provide any shear transfer and thus do not increase the stability of the modeled cage. While these simplified methods generally produce conservative results, it is beneficial to understand the varying level of conservatism each modeling method provides, and where a robust analysis may be more cost-effective.

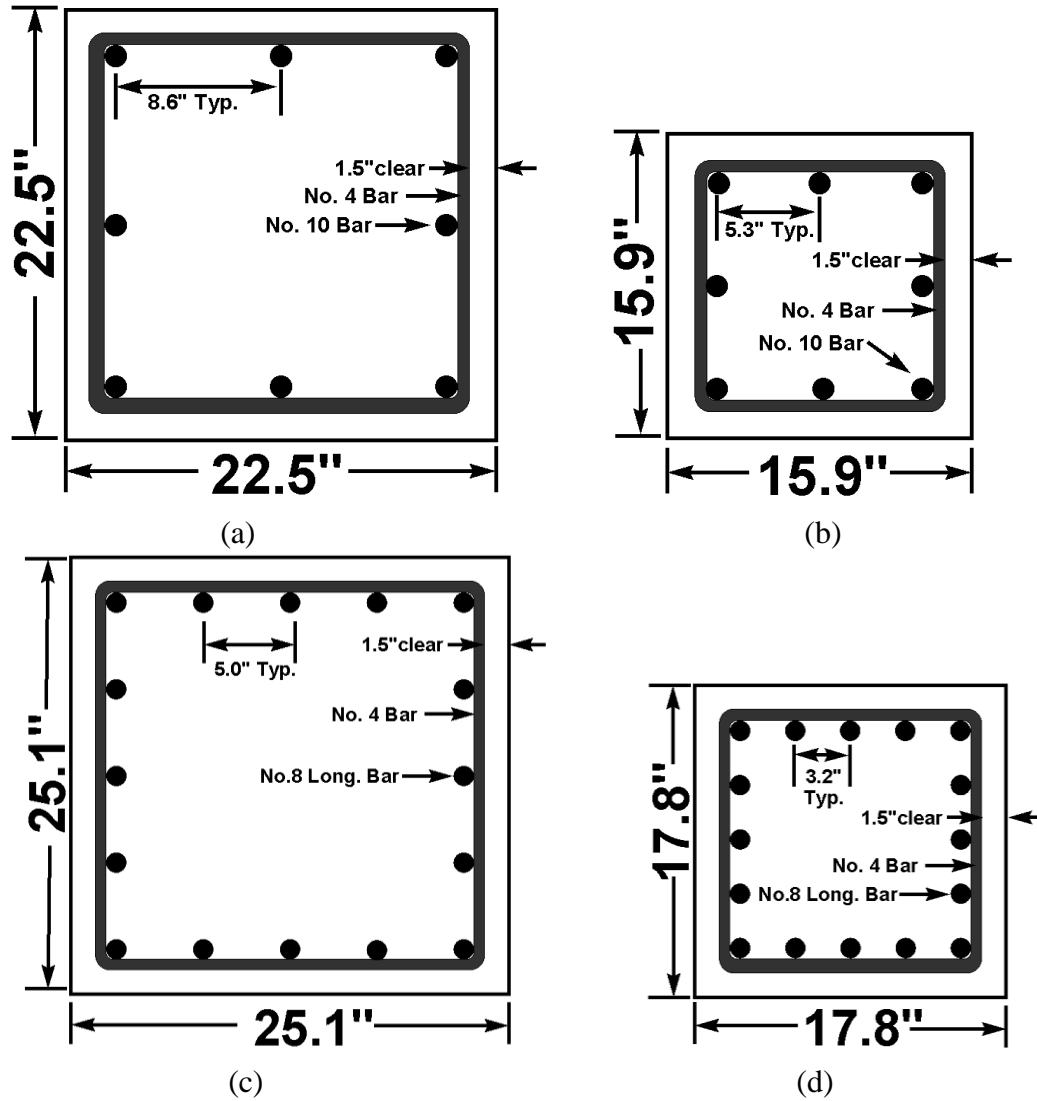


Figure 5: Column reinforcing layout for (a) (8)-#10 bars with $\rho=2\%$, (b) (8)-#10 bars with $\rho=4\%$, (c) (16)-#8 bars with $\rho=2\%$, and (d) (16)-#8 bars with $\rho=4\%$

Table 1: Column weights

Long. Bars	Tran. Spa. (in.)	ρ (%)	Longitudinal Steel Weight (lbs)	Transverse Steel Weight (lbs)	Total Weight (lbs)
(8)-#10	3"	2	1037.2	518.3	1555.5
(8)-#10	6"	2	1037.2	259.1	1296.3
(8)-#10	3"	4	1037.2	338.6	1375.8
(8)-#10	6"	4	1037.2	169.3	1206.5
(16)-#8	3"	2	1290.3	1178.2	2468.5
(16)-#8	6"	2	1290.3	589.1	1879.4
(16)-#8	3"	4	1290.3	777.3	2067.6
(16)-#8	6"	4	1290.3	388.6	1678.9

3.1.2 Bracing

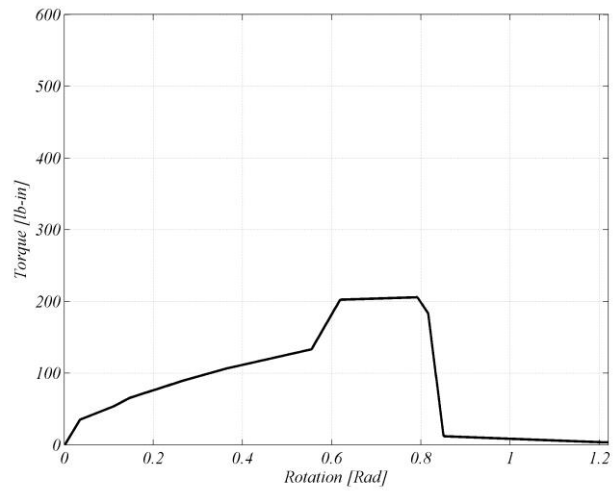
External bracing is applied at either the top or mid-height of the column in all models; reasonable bounds for the typical locations noted on construction sites. The robust analytical model provides physical elastic braces with sufficient rigidity (described in more detail below) while rigid boundary conditions are imposed for the simplified models. No internal bracing was used as a simplification for these analyses, which is a construction practice contrary to recommendations by Builes-Mejia.

3.1.3 Loading and Boundary Conditions

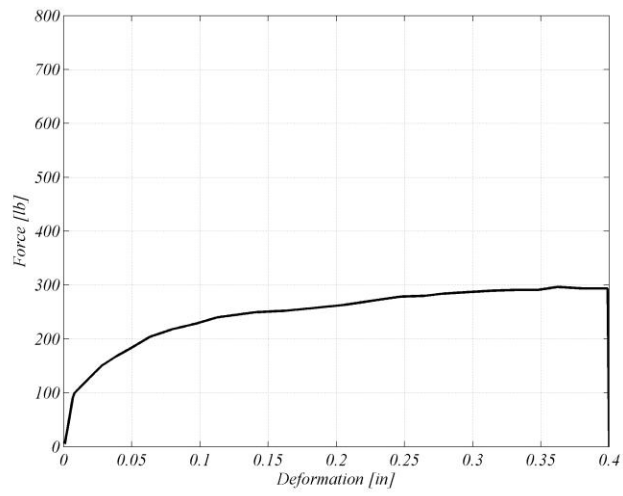
This paper focuses solely on gravity loading; i.e., lateral loading from wind or earthquake is not addressed. The boundary condition at the base of the column is varied as either fixed or pinned. Typical construction consists of dowels protruding from hardened concrete below and tied with tie wire to the column cage longitudinal reinforcement above. The actual base fixity lies somewhere between these two extremes, yet herein, the extreme conditions are analyzed rather than estimating the actual restraint.

3.1.4 Tie Wire

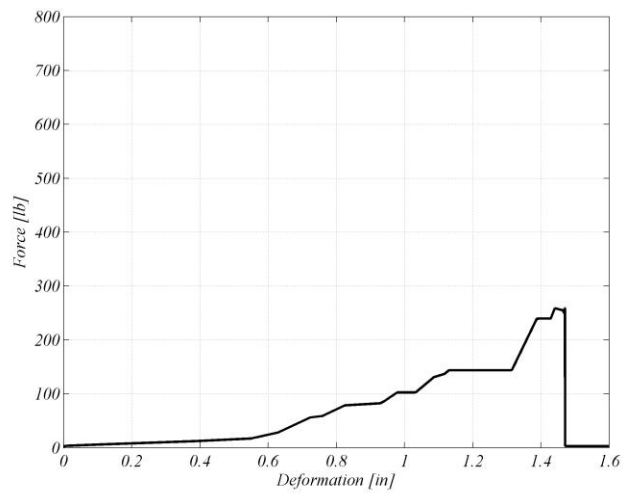
Most tie wire in the United States is subject to specification ASTM A 82. All ties are modeled assuming single-snap ties as tied by an experienced ironworker as tested by Builes-Mejia (2010). According to this reference, single-snap ties are one of the most common bar tying methods in California. As part of their study, the force-displacement characteristics of the bars were tested and characterized, and those results are used in the OpenSees model presented herein. The reader is referred to the referenced paper, specifically Fig. 3.29a, Fig. 3.7a, and Fig. 3.11a for more details. A plot of the moment-rotation ($M-\theta$), force-separation (ΔX), and relative translation of the bars ($\Delta Y, \Delta Z$) for the ties used in this research are shown in Fig. 6.



(a)



(b)



(c)

Figure 6: Single-snap tie wire: (a) moment-rotation $M-\theta$, (b) force-separation ΔX , and (c) relative translation $\Delta Y, \Delta Z$

3.2 Analysis Methods

Three distinct types of analyses are employed in this research to assess the structural stability of the column reinforcing cages: theoretical hand solutions based on a critical buckling load, a more refined analysis using Mastan2, and a robust finite element approach using OpenSees. This section details the analytical models and methods.

3.2.1 Theoretical Analysis Model

The simplest means to assess cage stability is to base solutions on the Euler buckling load. For these analyses, the area of the cage and the cage moment of inertia is the summation of each longitudinal reinforcing bar, and the weight of the cage is always assumed to act at the top node of the column. This method was chosen for two main reasons:

1. Applying a point-load at the top of the column will generally produce the lowest critical buckling load, and
2. Closed form solutions are readily available for top-loaded columns with various boundary conditions.

The result from this type of analysis is a critical load which can then be compared to the weight of the cage. For example, if the critical load is determined to be x and the cage weighs y , then the cage would remain stable so long as $x > y$. An engineer could use this simple hand calculation to quickly determine if the cage is at risk for instability. If so, then appropriate action could be taken to stiffen the section or a more robust analysis method could be employed.

3.2.2 Refined Analysis Model

Refined analyses are performed in Mastan2 (2010) version 3.3.1. Mastan2 is a free structural analysis software package that can solve for buckling loads by eigenvalue extraction or by second-order analysis considering geometric and material nonlinearities. Similar to the method used for the Euler buckling solutions, only one line of elements (single cross-section discretized into six equal length elements along the column's height) is modeled in Mastan2 with cross-section properties that are the summation of only the longitudinal reinforcing steel. One of the critical differences between analyses performed in this software versus the theoretical hand calculations is the distribution of weight. In Mastan2, the weight of the cage is distributed along the column height. To adequately account for the total weight of the cage listed in Table 1, an equivalent cross-sectional area (A_{equiv}) is deduced based on the column height and the density of steel as:

$$A_{equiv} = \frac{Total\ Weight}{\rho_s \times h} \quad (1)$$

where *Total Weight* is from Table 1, $\rho_s = 490 \text{ lbf/ft}^3$, and h is the column height (equal to thirty feet). It is this area that is used in the refined analyses.

The result from performing an elastic, eigenvalue buckling analysis is a load proportionality factor (LPF) that is a multiple (or fraction) of the cage weight at incipient buckling. That is, if the $LPF > 1$, then the column can at least support its own self-weight. Conversely, if the $LPF < 1$, then the column reinforcing cage is unstable under its own self-weight.

3.2.3 Robust Finite Element Analysis

The last model category explored in this study is based on a robust, three-dimensional, finite element analysis using OpenSees (2013) version 2.4.4, developed in part by the Pacific Earthquake Engineering Research Center. All elements utilized the co-rotational transformation from global to element local forces (i.e., a large-displacement formulation is implemented).

Longitudinal bars are modeled using displacement based, distributed plasticity elements with fiber cross sections to capture any potential instability due to individual or global interaction between axial and flexural forces. Each longitudinal bar is discretized at each transverse reinforcement location and contains three integration points along the length of each element for quadrature (i.e., the model with three inch transverse rebar spacing had twice the number of longitudinal elements as compared to the model with six inch spacing). Transverse reinforcement is modeled with elastic elements with section properties consistent with #4 reinforcing bar. Each tie element is modeled as a distributed plasticity displacement-based beam utilizing section properties from the force displacement relationships as discussed in Section 3.1.4 and illustrated in Fig. 6. In particular, the flexural properties are modified to obtain equivalent shears assuming double curvature over the length of the tie element.

Lateral bracing for the cage consists of a series of elastic, large-displacement truss elements for a total cross-sectional area of 10.0 in.² (i.e., three braces are used for the cages with (8)-#10 bars and five braces are used for cages with (16)-#8 bars). Based on the relative area to column cage properties, no significant deformations of the braces were observed (essentially, the braces act as rigid elements). Each brace extends out a distance equal to the height of the brace along the cage, creating a 45 degree angle with the ground. Brace elements are attached directly to the longitudinal bars at the edge of cage, and to a single point on the ground.

Initial imperfections consist of $L/500$ out-of plumb combined with $L/1000$ out-of-straightness between brace points. These numbers are not necessarily consistent with as-built cages, but are appropriate for relative comparisons with other models described above.

Static loading is applied at each longitudinal element and includes the proportional contribution from the transverse reinforcement. Fig. 7 contains typical displaced shapes for full- and mid-height braced column cages for Cases 27 and 29. Each figure depicts a vertical displacement at the top of the cage of one inch. All displacements have been magnified by ten.

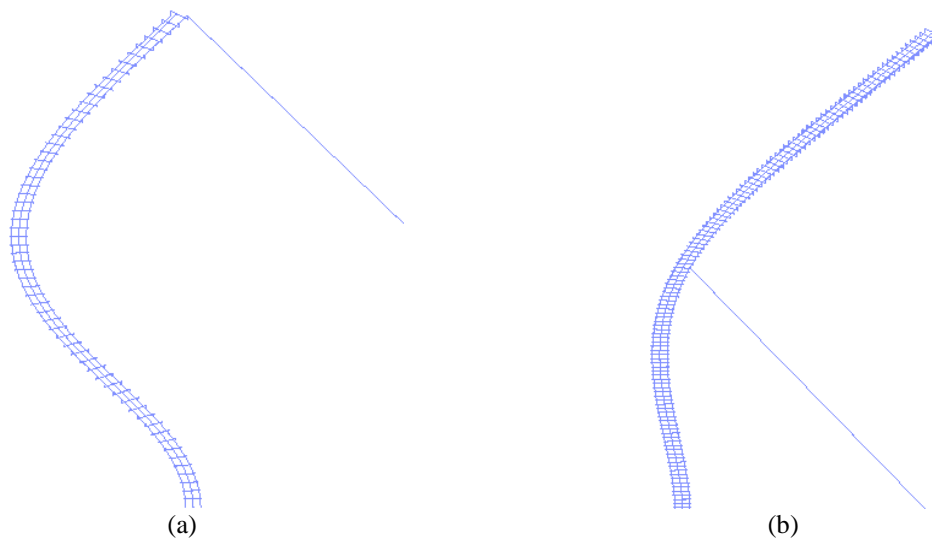


Figure 7: Displaced shapes (scaled 10x) for (a) bracing at L and (b) bracing at $L/2$

The force-displacement relationship for the top displacement versus the applied LPF for Case 1 is plotted in Fig. 8. The analysis is terminated after a drop in load, as shown below, and the peak force is recorded as the LPF in Table 2.

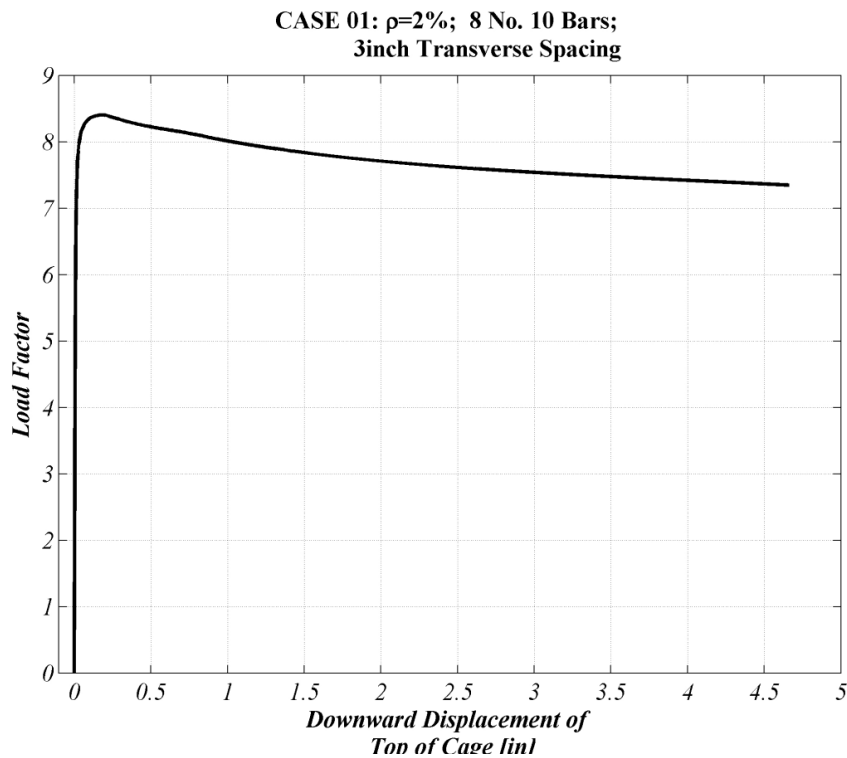


Figure 8: LPF versus downward displacement for Case 1

3.3 Analytical Test Matrix

Sixty-four analyses are performed in support of this research. The adjusted variables include:

1. The height of the bracing (at L or $L/2$)
2. The base fixity (either pinned or fixed)
3. The analysis type (theoretical, Mastan2, and OpenSees)
4. The ratio of reinforcement to concrete area ($\rho = 2\%$ or $\rho = 4\%$)
5. The size and layout of longitudinal reinforcement (either (8)-#10 or (16)-#8)
6. The spacing of the #4 transverse reinforcing bars (either 3" or 6")

For each scenario, the LPF is reported as a multiple of the total column reinforcing cage weight. The full testing matrix including results is shown in the next section.

4. Analysis Results and Discussion

The results from all sixty-four analyses are shown in Table 2. Some of the important observations from this study are discussed below.

The LPF always increases when comparing the Mastan2 results to the theoretical results.

For any comparison between similar test cases (e.g., Case 2 and Case 3), one notes that the LPF factor is higher for the analysis results from Mastan2 than from the theoretical analysis. This is likely the result of the manner in which the self-weight is applied. As mentioned in the preceding sections, for the theoretical analyses, the self-weight is “lumped” at the top of the column cage. Conversely, the Mastan2 models utilize a self-weight distribution along the column height.

For the case of a fixed base column that is free to move laterally at the top, any classic stability text (see, e.g., Timoshenko and Gere’s *Theory of Elastic Stability*, 1961) shows that the buckling load is:

$$(ql)_{cr} = \frac{mEI}{l^2} \quad (2)$$

where q is the distributed axial load (in pounds per foot), l is the column length, m is a factor equal to 7.84 for the boundary conditions described, E is the elastic modulus and I is the area moment of inertia. If one compares this to a similar case of a fixed base column which is loaded by a point load at the top and the top is free to move laterally, the factor m reduces to 2.47 ($\pi^2/4$). Therefore, a simple model which applies the mass of the column at the top leads to a reduction of the predicted buckling load by 68.5%, which may be considered as over-conservative and lead to potentially unnecessary bracing and time delays associated with installing and removing bracing during the erection sequence.

The LPF always increases when comparing the OpenSees results to the results from Mastan2.

Similar to the observation above, the higher fidelity finite element models in OpenSees predict a larger LPF of self-weight than predicted by Mastan2. The difference is mainly due to the interaction between the longitudinal and transverse reinforcing steel through the modeling of the tie wires, as discussed previously.

If the results of, e.g., Case 1 and Case 2 are compared, OpenSees predicts an almost 10% increase in buckling capacity. This would suggest that the interaction between the longitudinal and transverse reinforcement through the ties has an effect of increasing the moment of inertia of the cross-section roughly 10% over that of simply using the summation of the bars. The different moment of inertias for this specific section (8-#10 bars, $\rho = 2\%$) are:

- Considering no composite action – $I = \Sigma I_{bar} = 1.022 \text{ in.}^4$
- Considering complete composite action – $I_{composite} = \Sigma I_{bar} + \Sigma A_{bar} * d^2 = 564.6 \text{ in.}^4$ (551 times higher than no composite action)
- Considering OpenSees prediction – $I_{eff} = \Sigma I_{bar} * 1.1 = 1.124 \text{ in.}^4$

The results above suggest that going to the trouble of explicitly modeling transverse bars and tie connections yields a practically insignificant increase of 10% in the buckling compared to simply assuming the bars to be non-composite. Cases with significantly more ties exhibit more composite action (e.g., sixteen versus eight vertical bars increases the effective composite moment of inertia to 2.5 times versus 1.1 times).

Increasing the reinforcement ratio ρ decreases the capacity.

To change the reinforcement area to concrete area while maintaining the same amount of longitudinal reinforcing steel, it is necessary to reduce the bar spacing within the cross-section. For the cases with (8)-#10, increasing ρ from 2% to 4% coincides with a decrease of the bar spacing from 8.6 inches to 5.3 inches (see Fig. 5a and Fig. 5b). This decrease in spacing effectively reduces the fully composite moment of inertia from 564.6 in.⁴ calculated previously to 215.1 in.⁴, yet the capacity of the section increases (from an LPF of 8.4 to an LPF of 9.32, see Case 1 and 25, respectively). This initial, apparently counterintuitive result is due to the fact that the two cages have different weights. If one multiplies the LPF by the cage weight, then the overall load on the column cage is higher for the case where the transverse bars are spaced closer together.

As transverse bar spacing increases, results from OpenSees approach those of Mastan2.

For convenience of the present discussion, a subset of cases from Table 2 is shown in Table 3. If Case 1 is compared to Case 2, the increase of OpenSees's prediction over that of Mastan2 is 9.9%. However, in comparing Case 13 to Case 14, the difference in results is marginal. Similarly, the change in results between Cases 33 and 34 is 44.9%, whereas the difference between Cases 45 and 46 is 18.5%. The most-likely explanation for this observation is that as the transverse bar spacing increases, the effective composite action decreases. In the limit when the transverse spacing reaches the column height, the results are essentially identical. Similar results can be observed for cases with bracing at mid-height ($L/2$) of the column as in comparing Cases 7 and 8 to 19 and 20, as well as Cases 39 and 40 versus 51 and 52.

Table 3: Select cases highlighting differences resulting from varying transverse bar spacing

Case	L_b	Base	Analysis	ρ	No. Bars	Tran Spa	LPF
1	L	Fix	OS	2%	8 No. 10	3"	8.40
2	L	Fix	M	2%	8 No. 10	3"	7.64
13	L	Fix	OS	2%	8 No. 10	6"	9.18
14	L	Fix	M	2%	8 No. 10	6"	9.17
33	L	Fix	OS	2%	16 No. 8	3"	5.36
34	L	Fix	M	2%	16 No. 8	3"	3.70
45	L	Fix	OS	2%	16 No. 8	6"	5.76
46	L	Fix	M	2%	16 No. 8	6"	4.86

Similarly-reinforced columns with bracing at the top are able to reach higher buckling loads than columns with bracing at mid-height of the column cage.

The stability of columns is driven by second-order effects, i.e., secondary moments and displacements arising from primary forces acting through the displaced member geometry. The displaced geometry as it relates to stability can loosely be categorized as either $P-\Delta$ or $P-\delta$. $P-\Delta$ (commonly referred to as “large p-delta”) effects arise from primary forces acting through the displaced end points (or brace points) of the column. $P-\delta$ (commonly referred to as “small p-delta”) effects arise from primary forces acting through the out-of-plane displacement *between* end or brace points. Both of these effects will contribute to destabilizing the column.

In these examples, when the column reinforcing cage is braced at its top and loaded via a point load at the top of the column, the only secondary effects realized are those coming from $P-\delta$; since the end of the column cannot displace laterally (there are no $P-\Delta$ effects). Conversely, when reinforcing column cages in these virtual tests are braced at mid-height ($L/2$), there is a contribution from both $P-\Delta$ and $P-\delta$ effects to further destabilization of the column. This effect leads to different buckling capacities among similarly reinforced columns with varying brace height.

Table 2: Testing matrix

Case	L_b	Base	Analysis*	ρ	No. Bars	Tran Spa**	LPF
1	L	Fix	OS	2%	8 No. 10	3"	8.40
2	L	Fix	M	2%	8 No. 10	3"	7.64
3	L	Fix	T	2%	8 No. 10	3"	2.96
4	L	Pin	OS	2%	8 No. 10	3"	3.47
5	L	Pin	M	2%	8 No. 10	3"	2.74
6	L	Pin	T	2%	8 No. 10	3"	1.45
7	L/2	Fix	OS	2%	8 No. 10	3"	6.32
8	L/2	Fix	M	2%	8 No. 10	3"	4.37
9	L/2	Fix	T	2%	8 No. 10	3"	0.92
10	L/2	Pin	OS	2%	8 No. 10	3"	4.90
11	L/2	Pin	M	2%	8 No. 10	3"	3.31
12	L/2	Pin	T	2%	8 No. 10	3"	0.80
13	L	Fix	OS	2%	8 No. 10	6"	9.18
14	L	Fix	M	2%	8 No. 10	6"	9.17
15	L	Fix	T	2%	8 No. 10	6"	3.55
16	L	Pin	OS	2%	8 No. 10	6"	3.52
17	L	Pin	M	2%	8 No. 10	6"	3.29
18	L	Pin	T	2%	8 No. 10	6"	1.74
19	L/2	Fix	OS	2%	8 No. 10	6"	6.04
20	L/2	Fix	M	2%	8 No. 10	6"	5.24
21	L/2	Fix	T	2%	8 No. 10	6"	1.11
22	L/2	Pin	OS	2%	8 No. 10	6"	4.67
23	L/2	Pin	M	2%	8 No. 10	6"	3.97
24	L/2	Pin	T	2%	8 No. 10	6"	0.96
25	L	Fix	OS	4%	8 No. 10	3"	9.32
26	L	Pin	OS	4%	8 No. 10	3"	3.79
27	L/2	Fix	OS	4%	8 No. 10	3"	6.85
28	L/2	Pin	OS	4%	8 No. 10	3"	5.31
29	L	Fix	OS	4%	8 No. 10	6"	9.77
30	L	Pin	OS	4%	8 No. 10	6"	3.71
31	L/2	Fix	OS	4%	8 No. 10	6"	6.33
32	L/2	Pin	OS	4%	8 No. 10	6"	4.88

* T = theoretical, M = Mastan2, OS = OpenSees

** Tran Spa = Vertical spacing of #4 transverse reinforcing bars

Case	L_b	Base	Analysis*	ρ	No. Bars	Tran Spa**	LPF
33	L	Fix	OS	2%	16 No. 8	3"	5.36
34	L	Fix	M	2%	16 No. 8	3"	3.70
35	L	Fix	T	2%	16 No. 8	3"	1.43
36	L	Pin	OS	2%	16 No. 8	3"	2.63
37	L	Pin	M	2%	16 No. 8	3"	1.33
38	L	Pin	T	2%	16 No. 8	3"	0.70
39	L/2	Fix	OS	2%	16 No. 8	3"	5.16
40	L/2	Fix	M	2%	16 No. 8	3"	2.11
41	L/2	Fix	T	2%	16 No. 8	3"	0.45
42	L/2	Pin	OS	2%	16 No. 8	3"	3.91
43	L/2	Pin	M	2%	16 No. 8	3"	1.60
44	L/2	Pin	T	2%	16 No. 8	3"	0.39
45	L	Fix	OS	2%	16 No. 8	6"	5.76
46	L	Fix	M	2%	16 No. 8	6"	4.86
47	L	Fix	T	2%	16 No. 8	6"	1.88
48	L	Pin	OS	2%	16 No. 8	6"	2.51
49	L	Pin	M	2%	16 No. 8	6"	1.74
50	L	Pin	T	2%	16 No. 8	6"	0.92
51	L/2	Fix	OS	2%	16 No. 8	6"	4.72
52	L/2	Fix	M	2%	16 No. 8	6"	2.78
53	L/2	Fix	T	2%	16 No. 8	6"	0.59
54	L/2	Pin	OS	2%	16 No. 8	6"	3.66
55	L/2	Pin	M	2%	16 No. 8	6"	2.10
56	L/2	Pin	T	2%	16 No. 8	6"	0.51
57	L	Fix	OS	4%	16 No. 8	3"	6.25
58	L	Pin	OS	4%	16 No. 8	3"	3.03
59	L/2	Fix	OS	4%	16 No. 8	3"	5.90
60	L/2	Pin	OS	4%	16 No. 8	3"	5.53
61	L	Fix	OS	4%	16 No. 8	6"	6.35
62	L	Pin	OS	4%	16 No. 8	6"	2.74
63	L/2	Fix	OS	4%	16 No. 8	6"	5.10
64	L/2	Pin	OS	4%	16 No. 8	6"	3.96

5. Recommendations and Future Work

From the results presented herein, the following recommendations are offered for assessing column reinforcing cage stability:

1. For a preliminary assessment, simple hand calculations can be performed with the entire self-weight of the cage applied at the top of the column. This will produce a buckling load that is likely to be very conservative. If the capacity is found to be too low, the designer can modify the bracing or apply more refined analyses.
2. For cases that may be difficult to solve by hand or for those which the level of conservatism attributed to a simplified hand calculation is unacceptable, an analysis can be easily performed utilizing standard structural analysis software. (Mastan2 was used in this research, but any commercially available software that properly accounts for second-order effects could be used.) This method is thought to be a reasonable alternative to the robust method and removes a considerable amount of conservatism from simple hand calculations.
3. More closely spaced transverse reinforcing (or generally, more tie connections between transverse and longitudinal reinforcing) can help to increase the factor of safety against buckling of the column cage. The increase in transverse reinforcing and adequately constructed tie connections, increase the composite nature of the column by increasing the cage moment of inertia.

While this paper is aimed at exploring the basics behind column reinforcing cage stability under self-weight, significant additional work is required to assess column stability for a variety of other conditions not explicitly addressed herein. Other loads may be the result of, e.g., seismic demands, wind loading, and more interestingly, eccentrically applied worker loads. A forthcoming paper by the authors will address specifically the stability effects on column reinforcing cages loaded by ironworkers during the construction process.

Disclaimer

The views expressed herein are solely those of the authors and do not necessarily represent the position(s) of Exponent or any other individuals therein.

References

- ACI (2011). "Building Code Requirements for Structural Concrete", American Concrete Institute, Farmington Hills, MI. ACI 318-11.
- Builes-Mejia, J.C., Itani, A.M., and Sedarat, H. (2010). "Stability of Bridge Column Rebar Cages during Construction." Report Number CCEER 10-07, Center for Civil Engineering Earthquake Research, Department of Civil Engineering, University of Nevada. November.
- Casey, M.J. and Urgessa, G.S. (2013). *Rebar Cage Construction and Safety: Best Practices*. Construction Institute of the American Society of Civil Engineers. Published by American Society of Civil Engineers.
- Mastan2 (2010). Developed by R.D. Ziemian and W. McGuire. Version 3.3.1. www.mastan2.com.
- OpenSees (2013). "Open System for Earthquake Engineering Simulation". Pacific Earthquake Engineering Research Center. Version 2.4.4 (rev 5764). The Regents of the University of California. <http://opensees.berkeley.edu>
- Timoshenko, S. and Gere, J. (1961), *Theory of Elastic Stability*, New York: McGraw-Hill.